Journal of Computational Physics **157,** 280–301 (2000)
doi:10.1006/jcph.1999.6378, available online at http://www.idealibrary.com on IDEAL®

Comparison of Parametric and Nonparametric Methods for the Analysis and Inversion of Immittance Data: Critique of Earlier Work

J. Ross Macdonald

Department of Physics and Astronomy, University of North Carolina, Chapel Hill, North Carolina 27599-3255
E-mail: macd@email.unc.edu

Received June 2, 1999; revised September 14, 1999

Recently, two methods for the estimation of discrete and/or continuous distributions of relaxation times from small-signal electrical frequency-response data have been compared. For discrete-line distributions, the parametric method used was found to be inferior in some ways to the nonparametric one, which involved Tikhonov regularization, and it was concluded that the parametric one could not be employed to estimate continuous distributions at all. Here it is shown by Monte Carlo simulation that both conclusions are incorrect. The same data situations analyzed in the earlier work were reanalyzed using a complex nonlinear least-squares parametric method that has been employed to estimate discrete-line distributions since 1982 and continuous ones since 1993. Quite different results from those presented earlier were obtained, and the original parametric method was shown to be far superior to the nonparametric one for the estimation of discrete-line distributions, since inversion is unnecessary and resolution is far greater. For continuous or mixed distribution inversions, the parametric method was again superior, and it allows unambiguous distinction between discrete-line points and those associated with a continuous distribution, while the nonparametric inversion method does not allow such distinction and approximates all distributional points as continuous-distribution ones. The parametric method used and described here is also valuable for other data analysis tasks other than those involving inversion. Some of its error characteristics are investigated herein, and the importance of matching the weighting error-model to the form of the errors in the data is illustrated. It was found that with normally distributed random errors added to exact data, the distributions of estimated parameters were not normal but were closer to normal for proportional errors than for additive ones.

Key Words: inversion; deconvolution; regularization; parametric method; ill-posed problems; admittance spectroscopy; relaxation; data fitting; complex nonlinear least squares; dielectric spectroscopy.

0021-9991/00 $35.00

1. INTRODUCTION

For 10 years or more, two different methods have been used for inverting small-signal AC admittance data to obtain estimates of spectra, such as the deep trapping levels in a Schottky barrier or the relaxation-time distribution associated with the processes leading to the measured response. The frequency-response data considered here may involve discrete lines only, a continuous distribution, or a combination of both. One of the two deconvolution methods involves the use of Tikhonov regulation [1], and the other uses complex nonlinear least-squares fitting (CNLS) of an appropriate model [2–10]. Recently Maier, Winterhalter, and their associates have published three papers [11–13] dealing with the analysis of admittance data by a nonlinear Tikhonov regularization method (NTRM): termed by them a nonparametric method. The alternate CNLS parametric method (PM) developed by the present author [4] is mentioned in [11–13], briefly described in [12], and discussed, applied, and apparently compared in [13] to NTRM results for both simulated and experimental noisy admittance data, the latter for semi-insulating GaAs Schottky diodes. A list of acronym definitions is included at the end of this work.

The detailed comparisons of the usefulness of the NTRM and PM approaches carried out in [13] using Monte Carlo analysis of data with fairly low noise indicated that the NTRM was greatly superior to the PM for the inversion of a continuous distribution of relaxation times (DRT) and, as well, for a composite distribution containing three discrete lines and a continuous DRT. For the estimation of a DRT involving only three discrete lines, the PM results were superior except for uncertainty in the determination of the proper number of lines to estimate. Since these results differ greatly from those presented in much prior work using the original PM [4], further fitting and analysis is needed to resolve the differences.

Although the PM used in [13] was introduced by reference to that in [4], thus implying that the method was the same, this was not the case. Therefore, it is important to present DRT estimation results for the three DRT situations defined above using the original PM. Such results and their comparison with the NTRM and PM estimates of [13] are presented below. For easy distinction between the two PM approaches, let PMO denote the original version of [4] and PMW denote that used by Winterhalter *et al*. [13]. A very important unique feature of the PM is that it takes both the strength and position of DRT points as free parameters, not just the strength parameters as in other approaches.

Brief characterizations of the three methods are as follows:

- The NTRM is most appropriate for continuous distributions, although it was used for all three in [13]. Because the regularization term, which tames ill-posedness effects in noisy data, introduces a trade-off between the accuracy of a DRT estimate and its resolution, it rounds off any sharp corners of a distribution which may be present and necessarily represents a discrete DRT line as a much-broadened peak. The NTRM is appropriate when estimation accuracy needs to be sacrificed to obtain many-point high resolution of a continuous distribution.
- In [13] it is stated that "the parametric analysis is only suited for discrete distributions and cannot estimate continuous distributions at all," but the PMW is applied there to all three data situations. It leads to very poor results for continuous and mixed distributions. In addition, these poor results led the authors of [13] to conclude that the PM (actually the PMW) is unable to estimate reliable results for a composite distribution.
- The PMO applies to all three types of DRT situations and, as shown below, yields DRT estimates much superior to those of the NTRM for all three. For discrete lines only,

there are no noisy-data ill-posed effects, leading to exceptionally accurate, high-resolution DRT estimates with no broadening, even for appreciably noisy data. For continuous and mixed distributions, the PMO yields accurate point estimates of the distribution components and provides an unambiguous way of distinguishing between points associated with discrete lines and those belonging to a continuous distribution [2, 4, 7–10]. For low noise, it can represent sharp-corners without rounding, but as the noise level of experimental data increases, the number, M, of highly accurate continuous-DRT point estimates decreases. Thus, the resolution decreases with increasing noise. For large-noise continuous-distribution situations, such a those with relative errors greater than 5%, the NTRM approach is likely to be superior for most purposes.

Comparisons of the results of applying the PMO with those obtained in [13] for the other two approaches are presented below. All the present calculations were carried out with the free immittance-spectroscopy fitting/inversion computer program, LEVM [4, 14, 15]. Detailed discussion of the inversion procedures involved in the PMO and the PMW approaches is presented in the Appendix.

2. SIMULATION RESULTS

2.1. *Background*

Figure 1 shows the equivalent circuit used in [12, 13] to represent the Schottky diode and to generate frequency-response data from it. The C_i and R_i circuit elements, with $1 \leq i \leq M$, may represent the effect of deep levels, a continuous distribution, or both; C_{01} is a bulk geometric capacitance; and R_{01} accounts for non-zero dc conductance. The remaining elements may be identified as arising from electrode/interface effects. It is noteworthy that in his original admittance spectroscopy work, an important precursor of [11–13], Losee [16] did not include the R_{01}, C_{02}, R_{02}, and R_{03} elements of Fig. 1.

For all the present Monte Carlo simulations, we shall follow the procedure of [13] by first generating a simulated data set without added errors and then carrying out 1000 inversions of this set with independent random errors combined with the real and imaginary parts of each original data point for each of the MC replications. As in [13], the original 1000 random error sets were normally distributed with standard deviations of unity and means of zero. Then, from the individual free-parameter estimates of the 1000 inversions and their

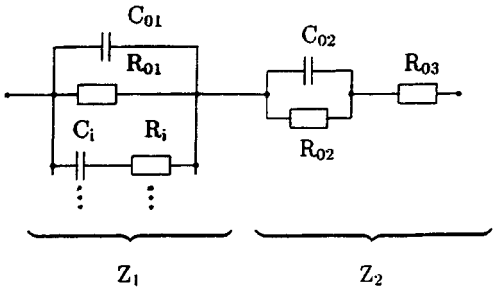

FIG. 1. Equivalent circuit used in Ref. [13] and herein to model the electrical response of a Schottky diode. The elements C_i and R_i, with $1 \leq i \leq M$, are included to represent the effects of deep levels, and are used here to represent discrete lines and/or continuous distributions of relaxation times. The other elements are identified in the text.

relative standard deviations of fit, S_F, the estimated parameter averages and relative standard deviations of these quantities are calculated. For simplicity $< >$ signs will be omitted since averages will be obvious.

Although the authors of [13] stated that their additive random errors corresponded "to a relatively constant error of 1%," they did not make it clear whether the 1% error applied to each of their individual data point values separately or to the overall relative standard deviation of the fit. For the first of these possibilities, the Gaussian-distributed random errors to be added are scaled by multiplying them by 0.01 times each individual real-part and imaginary-part data value, while for the second choice, all additive errors are scaled by a constant chosen to produce a value of S_F close to 0.01, a 1% relative error.

The type of error used is very important because proper analysis should use a weighting that matches as closely as possible the error character of the data. Thus, for the first choice above, proportional errors, one would use proportional weighting, PWT, while for the additive-error choice, unity weighting, UWT, would be appropriate, as demonstrated in Subsection 2.2. Unfortunately, the matter is further confused because the authors of [13] specify the use of PWT in their objective function, as in the earlier work of the author (e.g., [4, 6–10, 14, 15]), but they assume that their simulated experimental errors are relatively constant, an apparent inconsistency unless "relatively constant" meant constant relative to individual data values rather than approximately constant.

Judging from the results in [13], it appears that the authors may possibly have used additive errors rather than proportional ones, at least for their NTRM inversions. Because of this uncertainty, however, most of the present comparisons have been carried out both for additive errors and for proportional ones as well. In [13], N, the number of frequencies in a data set, was set to the large value of 200 for both NTRM inversions and for the PMW, but for the present PMO analyses, we use $N = 71$, for a range of ω_k from 1 to 10^7 rad/s with ten points per decade. In both cases, the ω_k values involved logarithmically scaled intervals.

The number of DRT points, M, is determined during the PM inversion procedure, but the fixed M value used in the NTRM analysis is not entirely clear. In [12] it is stated that M is at least 100. But in [13], the τ_i fixed-relaxation-time points are said to involve constant spacing within the range τ_{min}, τ_{max} of the distribution. If one takes $\tau_{min} \simeq 3 \times 10^{-6}$ and $\tau_{max} \simeq 1$ in order to cover most of the range of the full distribution involving three discrete points and a continuous contribution [13] and uses a spacing of 0.2×10^{-5}, required to yield enough points at the low end, then of the order of 10^6 points are required. Such a large value would lead to an extremely underdetermined least-squares situation, one mentioned in [13]. For usual least squares analysis, one wants the number of degrees of freedom to be positive, not the case for such a large number of fixed τ_i values. Although the introduction of a regularization term ameliorates this problem, it nevertheless seems likely that in [13] the authors used not more than about 100 fixed τ_i values, distributed with equal intervals on a logarithmic scale, certainly not constant spacing.

For the present PMO analyses, define the ith DRT point by the pair $\{e_i, \tau_i\}$, where e_i is a normalized strength parameter and τ_i specifies the position of the point [4]. For discrete DRT points, take $e_i = d_i$, and for points of a continuous DRT set $e_i = c_i$, since the discrete character of numerical analysis requires that even a continuous distribution must be defined by a finite number of discrete points. The PMW approach involves only the choice $e_i = d_i$, but the PMO may involve general $\{e_i, \tau_i\}$ pairs, possibly even including a combination of d_i and c_i points, a composite DRT. Because both e_i and τ_i parameters are taken free to vary during a PMO CNLS fit, much more accurate results are obtained than if the τ_is were fixed,

and a unique method of distinguishing between discrete DRT lines and continuous DRT points is available, as demonstrated below.

2.2. *Three Discrete DRT Pairs and Error-Model Results*

The simulated data sets here involve three $\{d_i, \tau_i\}$ distribution pairs, with values selected to agree with those of [13], plus all five of the remaining circuit elements of Fig. 1. But because the authors of [13] present their estimated DRT strength parameters in unnormalized form, for ease of comparison we shall do likewise, using the unnormalized strength quantities h_{ei} in place of the e_i ones. See the Appendix for their relationship. In [13], h_{di} is denoted by just h_i and h_{ci} by $\tau_i h(\tau_i)$. No explicit values of the latter quantity are presented in [13] except in plots. In all the h_{ei} plots in [13], a scale factor of 10^{-9} has been omitted without explanation, but it does appear in the corresponding plots in [12]. Note that $\{h_{ci}, \tau_i\}$ represents a discrete point of the $F(y)$ DRT of Eq. (A.1) when $F(y)$ represents an unnormalized continuous distribution.

Table I shows some results for the present discrete DRT situation. Scaled exact quantities are shown in the third column and 1000-replication Monte Carlo averages in the other columns. Note that the $M = 2$ values in column 4 agree poorly with the corresponding exact results (even though most of their estimated relative standard deviations are quite small!), and the S_F value is appreciably larger than it should be. By contrast, the correct

TABLE I

Comparison of Monte Carlo Estimated Parameter Values Obtained from Simulated Admittance Data with Three Discrete Deep Levels and the Five Non-distribution Circuit Elements of Fig. 1

Row	Parameter	Exact	UFit: M = 2	UFit: M = 3	UFit: M = 4	PFit: M = 3	NTRM
A	$100\ S_F$	∼0	2.26|0.065	0.994|0.32	1.001|0.32	0.998|0.064	∼1
B1	$10^{10}h_{d1}$	2	$4.87\|3 \times 10^{-4}$	2|0.0036	2|0.0037	1.97|0.24	1.5|0.13
B2	$10^{5}\tau_1$	1	$3.06\|2 \times 10^{-3}$	1|0.0033	1|0.0038	1.08|0.40	1.02|0.2
C1	$10^{10}h_{d2}$	3	—	3|0.0018	3|0.0019	3.02|0.11	3.3|0.06
C2	$10^{4}\tau_2$	1	—	1|0.0018	1|0.0018	1.03|0.09	0.97|0.41
D1	$10^{10}h_{d3}$	6	$6.29\|2 \times 10^{-4}$	$6\|4 \times 10^{-4}$	$6\|4 \times 10^{-4}$	6.02|0.022	6.2|0.11
D2	$10^{3}\tau_3$	1	$0.872\|5 \times 10^{-4}$	$1\|6 \times 10^{-4}$	$1\|6 \times 10^{-4}$	1.004|0.018	1.0|0.01
E_1	$10^{12}h_{d4}$	—	—	—	9.9|1.7	—	—
E_2	$10^{9}\tau_4$	—	—	—	9.8|8.2	—	—
O	$10^{10}C_{01}$	1	0.72|0.0014	1|0.0017	0.90|0.18	0.989|0.16	0.95|0.07
P	$10^{8}G_{01}$	1	1.05|0.0016	1|0.0017	1|0.0017	1|0.0026	0.999|0.002
Q	$10^{11}C_{02}$	1	$1.04\|2 \times 10^{-4}$	$1\|10^{-4}$	$1\|10^{-4}$	1.004|0.018	1.006|0.008
R	$10^{6}G_{02}$	1	$0.987\|9 \times 10^{-5}$	$1\|10^{-4}$	$1\|10^{-4}$	1.003|0.01	1.01|0.005
S	$10^{3}R_{03}$	1	$1.0000\|10^{-5}$	$1\|10^{-5}$	1|0.0014	1|0.0075	0.995|0.009

Note. Results are listed for runs with 1000 samples of additive or proportional independent Gaussian-distributed random errors in both real and imaginary parts of each data set. The Gaussian scale factor for additive errors was 8.075×10^{-11} Farads (UFit results), and that for proportional increments (PFit) was 0.01. Here S_F is the average relative standard deviation calculated from each set of 1000 replications, and the C(F), G (mhos), and R (ohms) parameters are defined in Fig. 1 with $G_{0i} = 1/R_{0i}$. The h_{di} and τ_i dielectric DRT parameters are the Fig. 1 quantities C_i and R_iC_i, respectively. The NTRM (nonparametric) results are taken from Ref. [13] and may possibly involve additive errors. A quantity, such as q, whose exact value is q_0, shown above without decimal places satisfies $0.9999q_0 < q < 1.0001q_0$ and is usually appreciably closer. For results shown as A|B, A is the estimated average value and B is the estimated average *relative* standard deviation of A.

$M = 3$ choice of column 5 yields virtually exact parameter estimates. Incidentally, the UFit S_F value of 0.994% could have been made 1.0% by using a slightly larger value of the random-error scaling factor.

For $M = 4$, nearly all of the parameter estimates are still accurately estimated, but the $i = 4$ ones of rows E_1 and E_2 are both very much smaller than the other discrete estimates (compare the scaling factors in column 2), and their relative standard deviations are so large that these estimated quantities cannot be statistically distinguished from zero. These results show that $M = 3$ is indeed the correct choice and that it is unnecessary to use a larger value.

The results presented in column 7, for proportional errors and proportional weighting (PWT), show appreciably poorer parameter estimates and relative standard deviation estimates than do those for additive errors when $M = 3$. This is because added proportional errors affect all the data while the present additive ones are so small that they affect primarily only the smaller data values. Finally, the results of column 8 should be compared with those of columns 5 and 7. We see that many of the Ref. [13] NTRM estimates are poor and show appreciable bias, as well as far greater uncertainties than do the discrete-DRT UFit estimates of the PMO. Although the $M = 3$ PMW results presented in [13] for the present situation are better than the NTRM ones, the relative standard deviations of their 11 parameter estimates are orders of magnitude larger than those of column 5. Further, there are very significant differences between the present $M = 4$ h_{di} results in column 6 and the corresponding PMW estimates in [13], all of which are very poor. For example, for $10^{10}h_{d3}$ the authors of [13] cite a value of 4.5|0.4 and for $10^3\tau_3$ a value of 0.72|0.4. In addition, their estimated values for the corresponding $i = 4$ quantities are 2.5|1 and 0.82|0.1, the latter value being significant even though it should not be.

The value of S_F and the corresponding O_M objective function of Eq. (A.4) will decrease as M is increased to $M + 1$ as long as adding another $\{e_i, \tau_i\}$ pair improves the fit. In many PMO fits of the author, it has been found that in this region O_M/O_{M+1} lies in the range from about 1.5 to 4, and O_M is approximately a decreasing exponential function of M. For the PMW procedure of [13], the criterion $O_{M+1} < 1.01O_M$ was introduced and was applied to each individual fit during MC analysis. When it failed, M was increased until $O_{M+1} \geq 1.01O_M$. For the present discrete-distribution situation this procedure led to 920 $M = 3$ results and 80 $M = 4$ ones [13]. Here we do not use this criterion but instead the more stringent one of comparing the results for all 1000 replications for each of the three M choices in the table, a comparison which makes it virtually certain that the $M = 3$ one is the proper one even if the exact parameter values were unknown, as they always are for experimental data.

Note that the relative standard deviation estimate of S_F is 0.32 for both the $M = 3$ and 4 PMO choices. This relatively large value means that some of the individual S_F values during a run of 1000 fits will be as large as 1.5% (or as small as 0.5%) and would thus be likely to require, in the PMW approach of [13], that M be incremented, and such fits would therefore not be counted as part of the Monte Carlo analysis for that value of M, censoring and thus biasing the results. Therefore, the present method of choosing an appropriate M is to be preferred. Further, determination of the proper value of M for an individual experimental data set, the usual problem, will again generally lead to an unambiguous choice, one based on comparing changes in parameter estimates and their standard deviation estimates, an integral part of the output of LEVM fitting, as M is incremented.

The results presented in Table I suggest that the present discrete PMO approach produces far better estimates than does the NTRM. The latter yields not a single line, when one is

present, but a continuous distribution which is approximately centered on the proper line. It is necessary to carry out separate integrations over the region of the resulting continuous distribution around the peak in order to obtain NTRM estimates such as those in column 8 [13]. This procedure is completely inadequate when two or more lines are close together, but such situations are handled accurately by the PMO approach [4].

The authors of [13] correctly state that in real materials instead of a single relaxation time for a deep level one should expect a broadened line. They do not, however, estimate such broadening, and it is clear that their line widths, which are about half a decade, are many orders of magnitude greater than is physically likely, and an unbroadened-line approximation will generally be most appropriate. Thus, it is clear that the PMO approach is to be preferred to the NTRM one for slightly broadened discrete-line situations. The PMO has been used to compare the inversion of a single line and a broadened but narrow (continuous) approximation to it in [5]. Incidentally, the tentative suggestion in [4] that it might be possible to combine the variable-τ feature of the PM with regularization is inappropriate since the standard regularization approach requires a fixed set of τs.

Because some consideration of the NTRM error model has been presented in [17], it is worthwhile to investigate aspects of the error models used here for the PMO approach, even though PMO inversion for experimental and simulated data containing errors has been presented in Refs. [3–10, 14,15, 18–20], and Monte Carlo analysis of LEVM fitting possibilities appears in [15, 18–20]. In particular, bias generated with different weightings is studied in [20] and the adequacy of correlation estimates in [19]. Finally, [15] contains a MC study of radioactive decay involving both experimental and simulated two-component exponential decay.

Figures 2 and 3 show some results of single fits of data defined as above with different types of added error and different weighting used in the fits. For the additive-error situations of Figs. 2a and 3a, we plot the unweighted (UWT) fit real and imaginary residuals versus the individual scaled pseudo-random errors which were added to the real- and imaginary-part data for each point. For the AU situation of Fig. 2a, where the weighting is appropriate

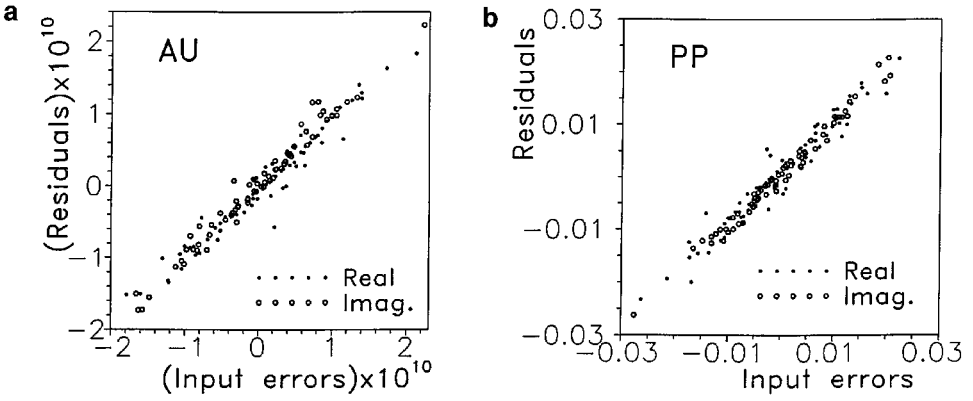

FIG. 2. Weighted real- and imaginary-part single-fit residuals versus the specific random errors which were directly (A) or proportionately (P) added to initially noise-free data calculated from the circuit of Fig. 1 with three discrete lines present. For the AU results in (a), unity weighting was used in the data fitting, while for the PP results shown in (b) proportional weighting was employed. All individual and Monte Carlo fit results plotted in the present work were obtained using the parametric method (PMO) described herein and instantiated in the LEVM fitting program.

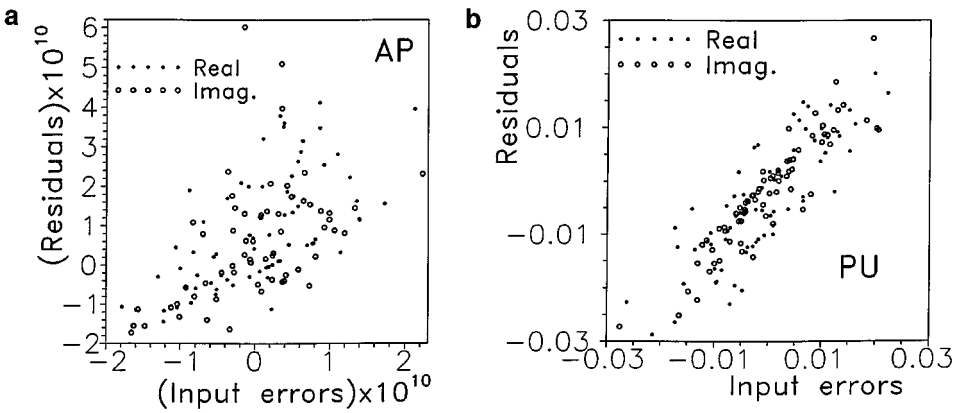

FIG. 3. Weighted real- and imaginary-part single-fit residuals versus the specific random errors which were directly (A) or proportionately (P) added to initially noise-free data calculated from the circuit of Fig. 1 with three discrete lines present. For the AP results in (a), proportional weighting was used in the data fitting, while for the PU results shown in (b) additive weighting was employed.

for the type of input errors, we see that the real and imaginary residuals are each highly positively correlated with their individual input errors, with, in fact, correlations of 0.98 and 0.99, respectively, as one would expect for a good fit. The situation is far different when the weighting does not match the type of the added errors. Thus for the AP results of Fig. 3a, where proportional weighting was used for the fit, the correlations are only of the order of 0.5 or less. The results for proportional errors, presented in Figs. 2b and 3b, show similar results. When the errors and weighting matched, as in the PP situation of Fig. 2b, correlations of 0.97 and 0.99 were found, and when they did not, for the PU results of Fig. 3b, again the correlations were of the order of 0.5 or less.

Although the estimated parameter values and their estimated standard deviations are appreciably worse for both types of mixed fit than for AU and PP results, the PU parameter estimates were considerably poorer on both counts than the AP estimate. These results graphically indicate the importance of matching the type of weighting used with the type of errors present in the data. LEVM also includes the possibility of using weighting which assumes the simultaneous presence of both small additive errors (an error floor) and proportional ones.

Finally, standard statistical tests for normality, and quantile–quantile plots, showed, as one might expect, that the AU and PP residuals were distributed normally with very high probability, but those for the PU and AP fits were not. Further, such tests for the MC S_F estimate for the PP situation led to quantile–quantile curves which showed reasonable agreement with a Gaussian distribution except at the high end of the plots where larger values of S_F than predicted for such a distribution were apparent. In fact, a log-normal distribution appeared to be about as likely as a normal one.

Tests of MC parameter estimates, such as those presented in Table I, showed that they were far from normally distributed for additive errors and were often highly peaked, although the τ_i parameter estimates were generally closer to normal than the h_{di} ones. Further, parameter-estimate distributions were more normal for proportional than for additive errors. Even though the parameter standard-deviation estimates do not have their usual probability interpretation here, they are nevertheless useful for comparisons and to give a rough idea of the likely uncertainty of the parameters. Although estimated standard deviations of

parameters are presented in [13], possible limitations on their interpretation are not mentioned there.

In summary, for the present discrete-DRT situation one can readily determine, using the PMO, that value of M which accounts for all the discrete lines (or levels) present and find that further increase in M is nugatory (see also [4]). Because the problem is not ill-posed, the discrete DRT parameters and all others present are on a common footing, and the situation is just one of fitting, not inversion. Thus, it is inefficient, much more difficult, and much less accurate to use the large-M NTRM for discrete problems, ones where regularization is inappropriate and unnecessary.

2.3. *A Continuous Gaussian Distribution*

In Ref. [13], the authors compared their PMW and NTRM results using data generated from both a continuous Gaussian distribution in a logarithmic τ variable and the five additional circuit parameters of Fig. 1. Their distribution was stated to involve a DRT τ peak value, τ_p, of 0.05 and a variance, σ^2, of 2 [13]. Note that a Gaussian distribution involving a logarithmic variable, such as the present y one defined below, is not a log-normal distribution [21], but it has been used for many years in the present field and is included as a fitting function in LEVM [14, 22, 23].

A normalized, continuous Gaussian distribution of dielectric relaxation times, involving y, here defined as $\ln(\tau/\tau_p)$, and a variance of σ^2, may be written as

$$F_D(y) = \exp[-(y/\sigma)^2/2]/(2\pi\sigma^2)^{\frac{1}{2}}, \tag{1}$$

and its response at the admittance level, say $Y_G(\omega)$, is

$$Y_G(\omega) = i\omega\Delta C \int_{-\infty}^{\infty} \frac{F_D(y)\,dy}{[1 + i\omega\tau_p \exp(y)]}, \tag{2}$$

where for numerical calculations the limits of the integral rarely need to be larger than 5σ, and ΔC is a measure of the strength of the distribution (see the Appendix). To agree with the choices in [13], we set $\Delta C = 10^{-9}$, but in order to match the actual width of the distribution used in [13], we had to choose $\sigma^2 = 1/2$ instead of the variance value of 2 specified in [13]. The free parameters for Gaussian DRT fitting with LEVM are ΔC, τ_p, and $\phi \equiv 2^{1/2}\sigma$, equal to 1 for the above choice of σ.

Before using the PMO to invert noisy data involving a Gaussian distribution and the two free parameters C_{01} and G_{01} of the Fig. 1 circuit, it is of interest to analyze such data directly by fitting the data to a Gaussian-distribution model and carrying out a 1000-replication Monte Carlo analysis based on direct fitting of exact data calculated with LEVM with additive random errors added, as in the previous section. The following estimates were obtained for ΔC, τ_p, ϕ, C_{01}, and G_{01}, respectively: $0.9999 \times 10^{-9}|0.0055$, $0.04999|0.0081$, $0.9999|0.0071$, $10^{-10}| \sim 0$, and $1.0002 \times 10^{-8}|.0041$. These estimates involve direct fitting of a known model and thus do not involve inversion.

Table II shows some PMO Monte Carlo estimates. Although all points are shown in the subsequent plots, for simplicity and to allow some quantitative comparisons between different PMO fitting situations, only the three $\{h_{ci}, \tau_i\}$ estimates that include the one with largest h_{ci} are listed. No PMW $\{h_{ci}, \tau_i\}$ estimates were listed in [13]. Note especially the improvement in the present $\{h_{ci}, \tau_i\}$ estimates for the U fits as M is increased from 7 to 11.

TABLE II
Comparison of Monte Carlo Fit Results for Simulated Admittance Data Involving a Gaussian Continuous Distribution and Two Additional Parameters

Row	Parameter	Exact, M = 11	UFit: M = 7	UFit: M = 11	PFit: M = 11
A	100 S_F	~0	0.9950|0.298	1.028|0.318	1.065|0.063
J_1	$10^9(h_{c4}, h_{c6})$	0.8310	0.7390|0.052	0.8302|0.0026	0.8183|0.012
J_2	τ_4, τ_6	0.0327	0.0297|0.055	0.0326|0.0051	0.0321|0.032
K_1	$10^9(h_{c5}, h_{c7})$	0.9882	0.9830|0.062	0.9887|0.0076	0.9999|0.017
K_2	τ_5, τ_7	0.0547	0.0557|0.134	0.0548|0.0619	0.0537|0.010
L_1	$10^9(h_{c6}, h_{c8})$	0.6814	0.5341|0.163	0.6833|0.0123	0.7354|0.026
L_2	τ_6, τ_8	0.0925	0.1051|0.162	0.0924|0.0106	0.0869|0.041
O	$10^{10}C_{01}$	1	1	1	0.9998|0.0014
P	10^8G_{01}	1	0.9987|0.007	0.9982|0.007	0.9988|0.0036

Note. The two parameter symbols listed together in several rows above apply to the $M = 7$ and the $M = 11$ fits, respectively. Other information is the same as that listed in the heading of Table I except that here the Gaussian scale factor used for additive errors was 1.25×10^{-10} Farads for the UFit results. For comparison, NTRM results from [13] are $10^{10}C_{01} = 0.99|0.01$ and $10^8G_{01} = 1.0|0.002$. No NTRM $\{h_{ci}, \tau_i\}$ numerical values were included in [13] for the present case.

Although the present PMO approach is appropriate for both discrete-distribution and continuous-distribution data, see Eqs. (A.6) and (A.7), and least-squares fitting (especially with the τ_i parameters free as well as the h_{ci} ones) provides some regularization effect for ill-posed continuous-distribution estimation, one finds that as M increases the uncertainty in continuous-distribution parameter estimates and their estimated standard deviations will eventually stop decreasing and begin to grow as ill-conditioning effects increase. Thus the maximum resolution of PMO-distribution estimates decreases as noise in the data increases. For exact simulated data, however, one can usually obtain at least 19 points, all of them very accurate, except possibly those at the extreme ends of the distribution. For experimental data involving a continuous distribution, a value of M which yields optimum PMO inversion results may always be found by increasing M until parameter uncertainties stop decreasing. Further increase in M is counterproductive.

For the present noisy-data situation, it was found that no improvement occurred as M increased from 13 to 14, and the $M = 11$ choice yielded the most parameter estimates with adequately small relative standard deviations. Table II also indicates, as in the discrete case above, that the relative standard deviation estimates of the continuous-distribution parameter points are significantly poorer for the $M = 11$ data containing proportional errors than for the additive error ones. The PMW results of [13] for the present AU situation were greatly inferior to those obtained here, with most of the replications leading to $M = 5$ and only 1.5% of them to $M = 6$.

When the $M = 11$ results are compared, where possible, with the results cited above for direct fitting of the data with a known Gaussian model, one sees that the parameters and error estimates of the two incidental parameters are comparable, and the $\{h_{ci}, \tau_i\}$ parameter estimates shown in the table are excellent, indicating that for the present situation the continuous-distribution PMO inversion approach suffers negligibly from ill-posed-inversion limitations. But this conclusion is somewhat misleading: the number of significant parameter estimates which may be obtained is limited by noise in the data as mentioned above, and, as demonstrated below, the smaller the h_{ci}s, the poorer their AU-type estimates are.

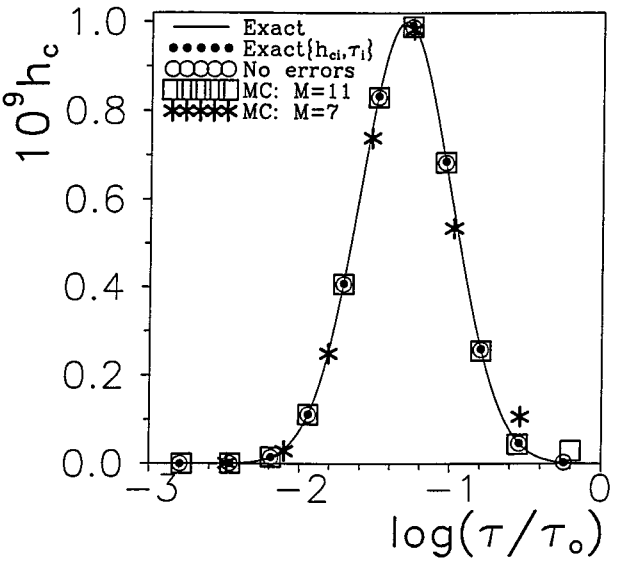

FIG. 4. Estimated Monte Carlo discrete points, h_{ci}, approximating a continuous Gaussian distribution of relaxation times included in Fig. 1 in place of its C_i and R_i elements. The peak of the exact input distribution occurred at $\log(\tau/\tau_o) = \log(\tau_p/\tau_o) = -1.30103$, with $\tau_p = 0.05$ s and $\tau_o = 1$ s. The latter normalizing value is used throughout this work. See Table II.

Furthermore, unlike the discrete-distribution situation, a small fraction of the present MC replications at fixed M did not fully converge after 900 or more iterations; therefore, only those that did were included in the MC results.

Figure 4 shows the estimated continuous-distribution points obtained from various fit choices. The solid line and the solid circles were calculated from the exact Gaussian DRT. The open circles, obtained from a single PMO fit of data without additive errors, should uniformly encircle the solid points if the estimates were exact. We see that, in fact, this seems to be the case, but the log–log plot of Fig. 5 shows that the two smallest h_{ci} estimates are slightly too large, possibly end-point artifacts of the quadrature weighting procedure used in the inversion [4].

The $M = 11$ AU points shown as squares in Fig. 4 also appear to be excellent estimates, except for the one for the largest τ. Note especially that the $M = 7$ points generally occur at different positions on the exact Gaussian response curve than do the $M = 11$ ones, contrary to the behavior found for discrete DRT points. Thus, it is clear that we are dealing here with points delineating a continuous rather than a discrete distribution, showing that the two can indeed be distinguished. No unambiguous discrimination of this kind is possible with the fixed-τ NTRM approach.

The NTRM curve in [13] corresponding to the one of Fig. 4 was plotted on a smaller scale than that of Fig. 4, but it nevertheless shows much larger discrepancies near its peak and also more errors on the high-τ side of the peak than those in Fig. 4. Although this continuous-DRT estimate was claimed in [13] to be very accurate, it is in fact much less accurate over the full τ range than that obtained with the PMO approach.

Log–log plotting, not included in the Ref. [13] work, is useful for showing the response in the small-h_e region. We see from Fig. 5 that the high- and low-τ end-points for both $M = 7$ and 11 are very poor, and, in fact, their relative standard deviations are greater than

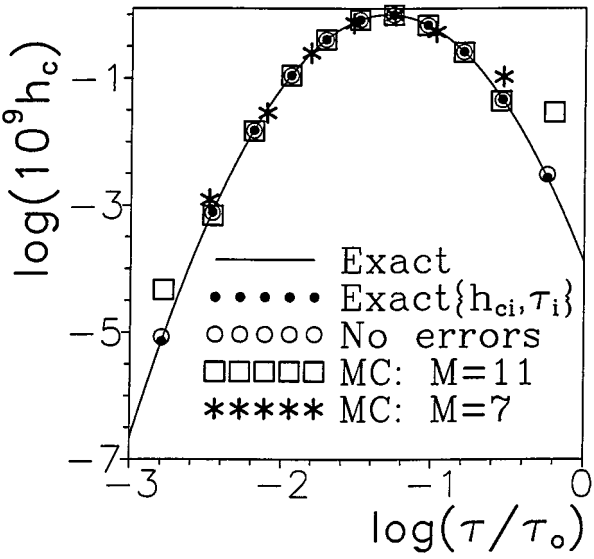

FIG. 5. The same results as in Fig. 4 but here plotted with logarithmic ordinate values.

one, indicating that these estimates are wholly inadequate. Thus, only $(M-2)$ points are meaningful for the present results. Nevertheless, they show that the PMO can indeed estimate a limited number of points of a continuous distribution appreciably more accurately than the NTRM can with a vastly larger number of points. This follows because regularization must try to achieve a balance between a good fit of the original data and not too much smoothing, something which renders most point estimates less accurate, even for the best choice of the regularization parameter, one not always readily obtained. Because the top nine open-square PMO points in Fig. 5 surround very closely the exact Gaussian values, denoted by the solid-circle points, it is clear that many points of a Gaussian distribution are extremely well estimated here from noisy data, as is also shown by separate direct least squares fitting of these nine open-square points to such a distribution.

In [13] it is implied that the least-squares estimator, such as that used in the PM and discussed in the present. Appendix, is not consistent for large M. Although the addition of a regularization term to the model, as in the NTRM, controls the ill-conditioning associated with large M values for a continuous distribution, it was not claimed in [13] that the NTRM is itself consistent. Consistency requires that estimated parameters, such the h_{ci}, converge in probability to their exact values as the number of observations, n, approaches infinity [24].

Here we find that the estimated uncertainties of the $n=1000$ PMO (mean) S_F values listed in Tables I and II are rather large and do not decrease appreciably for $n \geq 100$. Further, the estimated values of the h_{ci} uncertainties of Table II also do not decrease appreciably for larger n. Therefore, the nonlinear least squares estimator used in the PMO is indeed not consistent here for the inversion of continuous distributions, even for relatively small M values at constant N. But what matters most is that for M values large enough to give appreciable resolution, ill-conditioning effects are still minor for experimental data with usual small random errors, and many PMO DRT point estimates are quite accurate, as demonstrated by the results of columns five and six of Table II and by Fig. 5. It is finally worth emphasizing that when N is increased within a constant frequency range at

constant M, for an M value at or below its optimum value, MC analysis indicates that PMO parameter estimates approach their exact values as N increases, providing a possible means of achieving improved estimation accuracy.

2.4. *Three Discrete DRT Points and a Continuous Gaussian Distribution*

The results discussed in this section involve data sets which include the elements of both the preceding sections and the five non-distribution circuit elements of Fig. 1. Thus, for the PMO analysis when $M = 13$ there are a total of $2 \times 13 + 5 = 31$ free parameters. The more non-distributional extra parameters present, especially ones which contribute significantly to the frequency response in the same regions as the distribution, the less accuracy one can expect in inversion results. Thus, the continuous-distribution points in Table III and in Figs. 6 and 7 are less accurate than those listed in Table II and shown in Figs. 4 and 5. Nevertheless, Figs. 6 and 7 indicate that five or six good-point estimates of the Gaussian distribution are present for both the $M_c = 8$ and the $M_c = 10$ choices, where here M_c includes only the readily identified continuous-distribution $\{h_{ci}, \tau_i\}$ points out of the total $M = 11$ and 13 estimates shown.

For simplicity, the three discrete point estimates are not included in Fig. 7, but Fig. 6 and the results in Table III show that they are exceptionally accurately determined for both the M choices. Furthermore, since the positions of the discrete points were independent of M to three significant figures or more, unlike those of the continuous DRT, discrimination

TABLE III

Comparison of Monte Carlo Fit Results of Simulated Admittance Data with Three Discrete Deep Levels, a Gaussian Continuous Distribution, and the Five Non-distribution Circuit Elements of Fig. 1

Row	Parameter	Exact	UFit: $M_c = 8$	UFit: $M_c = 10$	NTRM
A	100 S_F	10^{-9}	0.998|0.24	1.021|0.24	∼1
B1	$10^{10}h_{d1}$	2	2|0.0059	2|0.0040	—
B2	$10^{5}\tau_1$	1	1|0.0031	1|0.0022	—
C1	$10^{10}h_{d2}$	3	3|0.0031	3|0.0024	—
C2	$10^{4}\tau_2$	1	0.9993|0.0051	0.9994|0.0047	—
D1	$10^{10}h_{d3}$	6	5.992|0.0042	5.994|0.0024	—
D2	$10^{3}\tau_3$	1	0.9991|0.0036	0.9986|0.0040	—
J_1	$10^{9}(h_{c4}, h_{c6})$	0.8980	0.7076|0.044	0.8991|0.021	—
J_2	τ_4, τ_6	0.0362	0.0281|0.074	0.0364|0.062	—
K_1	$10^{9}(h_{c5}, h_{c7})$	0.9558	1.004|0.034	0.9686|0.034	—
K_2	τ_5, τ_7	0.0611	0.0499|0.119	0.0614|0.125	—
L_1	$10^{9}(h_{c6}, h_{c8})$	0.5679	0.7521|0.077	0.5711|0.059	—
L_2	τ_6, τ_8	0.1054	0.0841|0.117	0.1045|0.074	—
O	$10^{10}C_{01}$	1	$1\|4.6 \times 10^{-4}$	$1\|2.6 \times 10^{-4}$	0.99|0.01
P	$10^{8}G_{01}$	1	0.996|0.015	0.994|0.019	1.0|0.002
Q	$10^{11}C_{02}$	1	$1\|4.7 \times 10^{-5}$	$1\|2.6 \times 10^{-5}$	1.0|0.002
R	$10^{6}G_{02}$	1	$1\|1.3 \times 10^{-4}$	$1\|10^{-4}$	1.01|0.005
S	$10^{3}R_{03}$	1	$1\|2.8 \times 10^{-5}$	$1\|2.9 \times 10^{-5}$	0.997|0.008

Note. Other information is the same as that listed in Table I except that here the Gaussian scale factor for additive errors was 2.35×10^{-10} Farads.

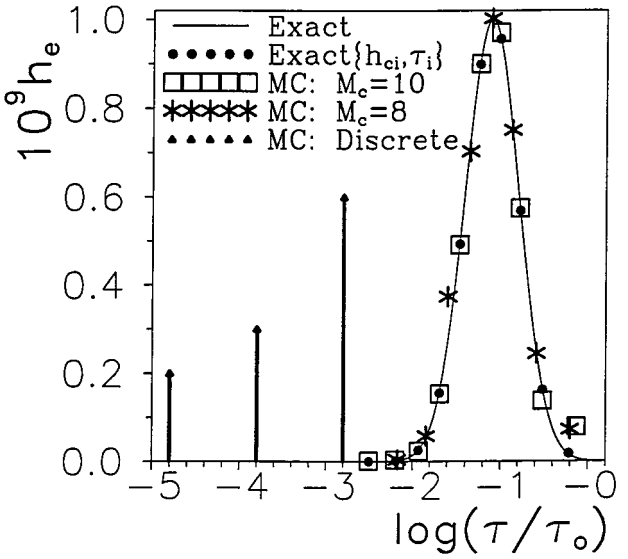

FIG. 6. Monte Carlo results for PM fitting/inversion similar to those in Fig. 4, but here the original data analyzed were calculated from the Fig. 1 circuit with three discrete lines, an exact continuous Gaussian DRT contribution, and all five of the other circuit elements shown in the circuit. See Table III. Here and in Fig. 7, M_C refers to continuous-distribution points only.

between the two types was unambiguous. It is worth reiterating that estimates of the discrete DRT points present here do not involve inversion problems when the PMO is employed since the fit model for discrete points of a composite distribution is exactly known. But, in contrast, PMO inversion of an unknown continuous distribution involves ill-conditioning associated with discretization and consequent inaccurate numerical quadrature, as well as

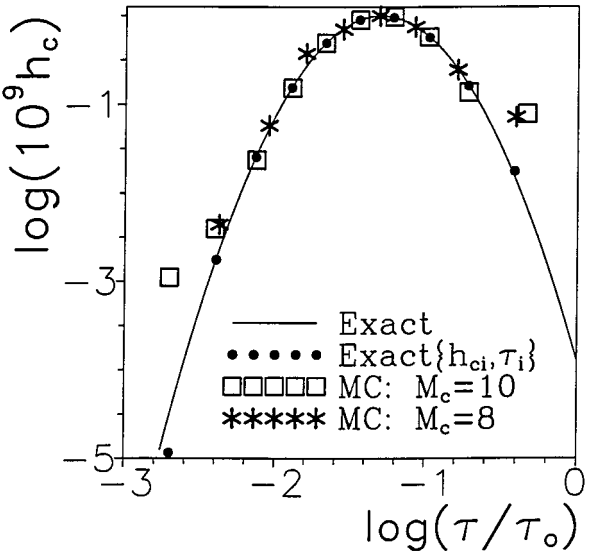

FIG. 7. Same results as in Fig. 6 but here plotted with logarithmic ordinate values and with discrete-line contributions omitted.

random errors in the data. Although the authors of [13] did not list any estimates of the five Fig. 1 non-distributional circuit elements for the present situation, they mentioned that they were nearly the same as those found for the continuous-distribution case. Therefore, those estimates are included in Table III.

Using their discrete PMW analysis approach and stopping criteria, the authors of [13] found that for the present data situation 92.5% of their 1000 replications involved only $M = 5$, and, of these five, only one defined the $\{h_{d3}, \tau_3\}$ point, and three others did a very poor job of delineating the continuous distribution. Better, but still poor, result were found with $M = 8$, but only 0.3% of the 1000 replications involved this choice. By contrast, the present $M = 11$ results are far superior to any of the Ref. [13] estimates for the present data situation and show clear distinction between the three discrete-distribution points and the eight points estimated for the continuous distribution. Even larger errors appeared for the NTRM continuous-distribution estimation of [13] than were present in the absence of discrete points, yet the authors again claimed very accurate estimation.

For actual GaAs measured data, the PMW analysis of [13] led to seven discrete-line contributions. The authors considered that six of these lines might be associated with a continuous, not discrete DRT, one which approximately defined an asymmetric, non-Gaussian distribution with a long tail on its small-τ side, a common shape. The seventh point agreed with a peak at even smaller τ also predicted by the NTRM analysis, but the question of whether it represented a discrete DRT point or not was unresolved. The results and comparisons herein indicate that had the PMO approach been used for these data, in place of the less appropriate models used in [13], it would most likely have been possible to resolve the above ambiguities by achieving both greater accuracy and definite discrimination. Then, not only would any discrete points be well identified but a good estimate of the actual continuous distribution present would have been found, and the procedure could have been applied for data at different temperatures in order to obtain useful estimates of relevant thermal activation energies.

3. SUMMARY AND CONCLUSIONS

By direct comparison of PM and NTRM MC results for the same data situations, nearly all of the criticisms of the PM in recent publications [12, 13] have been shown to be unfounded. The criticisms evidently arose, at least in part, from differences between the PMW approach employed in [13] and the PMO approach described herein and used previously. The PMO is far superior to all other analysis methods for estimating discrete-line contributions to data, since such estimation does not require inversion. By contrast, the NTRM greatly broadens delta-function lines and cannot distinguish them from narrow continuous distributions or resolve them when they are close together.

For the estimation of continuous or mixed distributions, the PMO has several advantages over the NTRM approach, particularly for admittance data, such as that considered here, which extends over many decades of frequency. First, it allows unambiguous identification of and discrimination between estimated points associated with discrete lines and those connected with continuous distributions. Second, it leads to more accurate determination of discrete-line points and of a limited number of continuous-distribution points than does the NTRM. As the noise present in the data increases, however, the number of significant continuous-distribution points which can be extracted by PMO inversion decreases. Nevertheless, for ordinary experimental data, much inversion experience using the PMO shows

that a sufficient number of significant points can be found to well define the distribution and identify it if it is of known form. For continuous distributions with many peaks and valleys (not the usual situation), however, the NTRM is likely to be able to delineate the distribution more completely when the noise level is relatively high than can the PMO approach. But, as usual for regularized inversion, one then trades off accuracy for resolution.

The LEVM computer program [4, 14, 15] allows one to use the PMO to fit or invert data at any of the four immittance levels and, more importantly, it allows one to estimate either a dielectric- or a conducting-system DRT. Such estimation may be carried out with full complex frequency-response data, with either the real or the imaginary part of such data, or from the associated temporal response data. Further, when the distribution has been estimated by one of these approaches, it can be used to calculate the response associated with any or all of the others. Thus, it obviates the need for Kronig–Kramers or Fourier transformation of the original data, an advantage which is especially important when the data span many decades.

Given some data, there are three distinct analysis avenues of usual interest. First, one may merely wish to obtain a function that fits the data as accurately as possible, perhaps for interpolation or extrapolation purposes. In this case, the PMO should be the method of choice, especially for low-noise situations. Usually more important is the task of fitting the data to a known model in order to estimate its parameters and to use the results to gain insight into the physical processes involved in the situation that led to the data. This approach allows one to discriminate between several plausible models, select the one which fits best, and evaluate the level of residual systematic error if it is significant [6, 7, 25–27]. The model used may or may not be defined in terms of a DRT. The LEVM program is particularly valuable for such fitting.

Finally, one may want to derive an estimate of the DRT inherent in the data or verify its presence. This approach is distinct from the ones immediately above only for continuous distributions. But even here, if one believes that a particular continuous distribution is likely, it is best (at least initially) to avoid inversion (but not ill-conditioning arising from discretization) and to fit the data directly with one or more response models involving the DRTs of interest. If a good fit without significant systematic error is obtained, one can stop the process there. If, however, one wishes to estimate an unknown continuous DRT from the data, inversion (such as that possible with the PMO or NTRM) may be necessary.

Although the titles of all three of Refs. [11–13] involve the subject of analysis of admittance data, it is worth pointing out that [11, 12] use a variant of the NTRM method and thus deal only with inversion approaches. The work of [13] includes a variant of the PM, as well as an improved version of the NTRM, but again both approaches are used to estimate DRT components. Therefore, it is only to the last of the three types of data analysis defined above that the [11–13] work primarily applies.

Definition of Acronyms

AP	Additive errors and proportional weighting (PWT)
AU	Additive errors and unity weighting (UWT)
CNLS	Complex nonlinear least squares
DRT	Distribution of relaxation times
LEVM	A complex nonlinear least-squares fitting and inversion program
MC	Monte Carlo analysis

NTRM	Nonlinear Tikhonov regularization method; see [1, 13]
PFit	Fit of data with PWT
PM	Parametric method: variable τ_is and no explicit regularization; the designation "PMO" refers to the original method (e.g., [4]), and "PMW" to that in [13]
PP	Proportional errors and proportional weighting
PU	Proportional errors and unity weighting
PWT	Proportional weighting in fitting
UFit	Fit of data with UWT
UWT	Unity weighting in fitting

APPENDIX: PMO AND PMW INVERSION APPROACHES

A1. *Background*

Parametric inversion/fitting approaches of the type considered herein involve the estimation of $2M$ $\{e_i, \tau_i\}$ parameters, since the τ_i, as well as the e_i, parameters are taken free to vary. As defined in Subsection 2.1, e_i is a general strength parameter which can represent discrete-DRT, d_i, or continuous-DRT, c_i, points. In contrast to "parametric," the term "nonparametric" is used in [12, 13] to indicate that the inversion procedure assumes the presence of a continuous DRT, even though numerical estimation, a necessary part of the approach, requires the replacement of integrals by sums and will yield only a finite number of points. Although the NTRM approach, which uses only fixed values of τ_i, can involve a very large value, M, of free c_i-parameter estimates, the term "nonparametric" seems a somewhat misleading descriptor, and the more specific designation, NTRM, is used in its place herein.

Rather than employing a large number of fixed τ_i values as in the NTRM, the PMO as used here and in earlier work (e.g., [4, 6–10]), usually starts with a small number, M, of free-parameter τ_i and e_i starting values, obtains an inversion solution, and continues obtaining such solutions with increasing M until the decreasing estimated standard deviations of the solution parameters finally reach approximate constancy or begin to increase. For simulated data without added errors, such termination is determined by round-off and truncation errors in the computations and data, and the standard deviation of the relative residuals of the fit, S_F, for either frequency- or time-dependent data is often as small as 10^{-8} or less, a far more accurate fit than is possible with the NTRM because of its regularization term. In contrast, the presence of experimental errors in the data leads to a smaller useful M_{max}, with the larger the errors, the smaller M_{max}.

A2. *Basic Equations and Minimization*

In order to provide an equation for the total admittance of the circuit of Fig. 1, $Y(\omega)$, we begin by considering the dispersive contribution associated with M $\{e_i, \tau_i\}$ pairs, where the e_i's are proportional to the C_i's and $\tau_i = R_i C_i$. We follow earlier work [4, 6–10] by defining U_n as an unnormalized measured or model quantity of interest, such as an impedance or complex resistivity, or a complex dielectric constant. Here, n is either taken as D, to denote dielectric dispersion, or 0 or 1, denoting two kinds of conductive-system dispersion. It is mathematically convenient to express the normalized form of U_n, I_n, in terms of a DRT, say

$g_n(\tau)$. Let $x \equiv \tau/\tau_{on}$, where τ_{on} is a characteristic response time of the fitting model or just a normalization quantity, and define $y \equiv \ln(x)$ and $G_n(x) \equiv \tau_{on} g_n(\tau)$. We may now write

$$I_n(\omega) \equiv \frac{U_n(\omega) - U_n(\infty)}{U_n(0) - U_n(\infty)} = \int_0^\infty \frac{G_n(x)\,dx}{[1 + i\omega\tau_{on}x]} = \int_{-\infty}^\infty \frac{F_n(y)\,dy}{[1 + i\omega\tau_{on}\exp(y)]}, \qquad \text{(A.1)}$$

where

$$U_n(\omega) = U_n'(\omega) + i\delta_n U_n''(\omega), \qquad \text{(A.2)}$$

and thus

$$I_n(\omega) = I_n'(\omega) + i\delta_n I_n''(\omega). \qquad \text{(A.3)}$$

Since the DRTs are taken normalized in the above, it follows that $I_n(0) = 1$ and $I_n(\infty) = 0$. It is important to emphasize that the choice $n = \mathrm{D}$ specifies that the U_D response of Eq. (A.1) refers to only that part of the complex dielectric constant $\epsilon(\omega)$ (or corresponding complex capacitance) associated with dispersion and thus can be represented by a distribution of dielectric-system relaxation times. On the other hand, the choices $n = 0$ and $n = 1$ specify response at the complex resistivity $\rho(\omega)$ (or impedance) level and thus involve, through G_0 and G_1, distributions of conductive-system relaxation times. We follow the usual sign conventions and set the quantities δ_0 and δ_1 in Eqs. (A.2) and (A.3) equal to 1 and δ_D equal to -1. Incidentally, the F_n distribution above may be simply related to a distribution of activation energies [28] and is given by $F_n(y) \equiv x G_n(x)$.

Although it has been shown that if a given data set may be well represented by a dielectric-system DRT, it can also usually be well represented by a conducting-system one instead [9]; we shall follow the work of [11–13] here and consider only dielectric dispersion, consistent with Fig. 1. We shall thus omit the D subscript from now on and take $I(\omega) = I_D(\omega)$. Let $\epsilon(0) - \epsilon(\infty) \equiv \Delta\epsilon$, an overall dispersion-strength quantity, and note that the dispersion contribution at the admittance level is just $i\omega C_V \Delta\epsilon I(\omega)$, where C_V is the vacuum capacitance of the system for unity dielectric constant. Then the sum of the C_i's is just $C_V\Delta\epsilon$. The $Y_1(\omega)$ part of the Fig. 1 circuit, equal to $1/Z_1$, is then given by $G_{01} + i\omega\{C_{01} + C_V\Delta\epsilon I(\omega)\}$. Here $C_{01} = C_V\epsilon(\infty)$, and $G_{01} \equiv 1/R_{01}$ should not be confused with the G_1 distribution defined above. Finally, the Z_2 of Fig. 1 is given by $(G_{02} + i\omega C_{02})^{-1} + R_{03}$, and $Y(\omega) = \{Z_1(\omega) + Z_2(\omega)\}^{-1}$. For convenience, explicit units will be suppressed herein, but the units of capacitances and resistances are all taken as Farads and ohms, respectively.

In this section, we shall use the normalized strength parameters e_i, but it is readily shown that the unnormalized NTRM strength parameters used in [12, 13], h_{ei}, are related to the corresponding normalized e_i ones by $C_V\Delta\epsilon e_i w_i = h_{ei} w_{Ti}$, where the w_i are the quadrature weights introduced in Eq. (A.7) below and the w_{Ti}'s are NTRM weights. If we assume that $w_i = w_{Ti}$, it follows that $\Delta C \equiv C_V\Delta\epsilon = \sum_{i=1}^M h_{ei} w_i$, and so $h_{ei} = C_i = \Delta C e_i$. For the discrete DRT situation, $h_{ei} = h_{di}$ and all the $w_i = 1$. For the NTRM, $e_i = c_i$.

In the present work, we shall use Y to denote model values and Y_d to denote data values. We calculate 1000 $Y(\omega)$ synthetic data sets each involving N discrete ω values using the Fig. 1 circuit (the model) without added error or with errors (then designated by $Y_d(\omega)$), and these data sets are inverted/fitted by the specific PMO approach instantiated in the LEVM computer program. Such inversions just amount to CNLS fitting of the model to the data in order to obtain estimates of the free parameter values of the model, many or all of which

may define a distribution of relaxation times such as that in Eq. (A.1). But nonlinear analysis is needed even in linear situations because all probability-density strength parameters are constrained to be positive. For a fixed value of M, the objective function which is to be minimized, O_M, is of the form [14, 15, 18]

$$O_M = \sum_{k=1}^{N} \left[(R'_k)^2 + (R''_k)^2 \right], \tag{A.4}$$

where $R'_k \equiv [Y'_{dk} - Y'_k]/V'_k$ and $R''_k \equiv [Y''_{dk} - Y''_k]/V''_k$ are weighted residuals. The actual weights involved in the fitting are $1/V'^2_k$ and $1/V''^2_k$.

LEVM allows many different types of weighting (error models) to be chosen (see, e.g., [14, 15, 18] and the LEVM manual). Here we need only consider unity weighting (UWT), where all the V's are set to unity, and proportional weighting (PWT), where $V'_k = Y'_{dk}$ and $V''_k = Y''_{dk}$ for all k values. If we define $D \equiv 2N - M_T$ as the number of degrees of freedom for a fit of complex data, then the variance of the fit, S_F^2, is just given by O/D. This is a standard and common definition of the variance, generalized to complex-data fitting [14, 15, 19]. Although presmoothing of data before least-squares fitting is mentioned in [4] and may possibly be useful for very noisy and irregular data, it should generally be avoided since the least-squares fitting itself provides a kind of smoothing.

For complex data fitting, M_T is the sum of $2M$ and the number of all other free parameters of the fit. Note that S_F is the standard deviation of the relative residuals for PWT and is thus actually the relative standard deviation of the fit. Even in the UWT case, we calculate such a relative standard deviation for comparison with PWT values. That S_F is indeed a proper measure of the relative standard deviation of the weighted fit is shown by the S_F estimates for Monte Carlo fits of data with known variance listed in Tables I–III herein, as well as by many prior Monte-Carlo fit results.

A3. *Discrete, Continuous, and Composite Fitting Models*

It remains to discuss the numerical calculation of $I(\omega)$. To do so for discrete data, $\omega_{min} \le \omega_k \le \omega_{max}$ with $1 \le k \le N$, one must approximate the integrals in Eq. (A.1) by numerical quadrature. This is trivial for a purely discrete distribution involving delta-function lines because then, for example, [4, 6],

$$G(x) = \sum_{i=1}^{i=M} d_i \delta(x - x_i), \tag{A.5}$$

and so

$$I(\omega_k) = \sum_{i=1}^{i=M} \frac{d_i}{[1 + i\omega_k \tau_i]}, \tag{A.6}$$

an exact result with no τ_i discretization errors involved. Here $\omega_k \tau_i$ may be written as $(\omega_k \tau_o)(\tau_i/\tau_o) \equiv \Omega_k x_i$. For experimental or synthetic immittance data it is conventional to use N ω_k data points distributed equally or approximately equally on a logarithmic scale between ω_{min} and ω_{max}. The PMW approach in [13] involves equations equivalent to Eq. (A.6).

The situation is slightly more complicated for continuous or mixed distributions. In [13] the authors use only their equivalent of Eq. (A.6) for their PMW approach, one only appropriate for discrete distributions, although they applied it to continuous ones as well. A straightforward approach for continuous or composite distributions is to initially ignore the difference between any d_i and c_i strengths present and use an appropriate quadrature approximation for the integral of Eq. (A.1), one which involves the weights w_i. The result, written in terms of y_i, is

$$I(\omega_k) = \sum_{i=1}^{i=M} \frac{e_i w_i}{\left[1 + i\omega_k \tau_o e^{y_i}\right]}. \tag{A.7}$$

This result reduces to that of (A.6) when all the quadrature weights are set to unity, but remember that the τ_i's are *not* distributed with constant spacing, as is the case for the present PMO and the PMW, which both take the τ_i's as free parameters. Nor is constant spacing present for the NTRM of [13] which uses fixed τ_i points, apparently distributed uniformly on a logarithmic scale. To treat these situations properly a special generalized quadrature procedure is needed, as described in [19]. When Eq. (A.7) is used for a possibly composite DRT, it is easy to distinguish d_i and c_i points, as discussed and demonstrated in the main text.

In [11–13] the authors used expressions similar to Eq. (A.7) as that part of their NTRM analyses which did not include their regularization term. But in [11, 12] they omitted any quadrature weights for these analyses and instead used their equivalent of Eq. (A.6). They thus implicitly estimated discrete rather than continuous distributions. It is only in [13] that w_i terms appear, in consonance with the earlier approach of [4]. That earlier work is not mentioned at this point nor is the change from the earlier analysis methods of [11, 12] noted. In [13] the authors do, however, identify the weights as arising from the discretization but do not discuss their calculation. In contrast, in [4] and in the LEVM manual several specific quadrature procedures and the resulting weights associated with them are discussed.

It is worth mentioning that when a converged inversion of data to yield a DRT estimate has been carried out using either Eq. (A.6) or (A.7), that solution is readily converted, using LEVM with minimum additional calculation, to the one involving the other expression. Note, however, that conversion of the point estimates of a true continuous distribution, where estimation is ill-conditioned and ill-posed, to Eq. (A.6) points is not physically meaningful.

On the other hand, a $\{d_i, \tau_i\}$ fit of data involving a continuous distribution provides an approximation to the appropriate set of $\{c_i, \tau_i\}$ points defining the distribution. Once a distribution has been accurately estimated and is available in either numeric or analytical form, it can be used to transform response from the frequency to the time domain or vice versa [6]. This capability is particularly valuable for data spanning many decades, a situation where numerical Fourier transformation is usually impractical [2, 4, 6].

Incidentally, CNLS fitting of equations equivalent to (A.6) with all parameters free to vary has been used since the early 1980s [29], but such PM analysis involving Eq. (A.7) seems to have been first introduced in 1993, the PMO [4]. An approach equivalent to the use of Eq. (A.6) with all d_i and τ_i parameters free, together with nonlinear least squares fitting, was independently described in 1989 for viscoelastic situations [30]. The requirement that all e_i and τ_i parameters be positive, necessary for a physically realizable probability density, was not mentioned in [13, 30]. All the present dispersion approaches are applicable to mechanical as well as electrical dispersion/relaxation situations.

How can one explain the differences between the PMW, PMO, and NTRM results, particularly those for continuous and composite distributions? First, the PMO and PMW involve the unique feature of allowing the τ_i parameters to be free variables during fitting [4]. Second, the PMO uses a very stringent double-precision iterative convergence criterion, namely that convergence is not declared until changes in the objective function only occur at the 11th decimal place or beyond. Third, since the PMW approach does not employ quadrature weights at all when it is used for continuous distributions and the NTRM may not use quadrature weights appropriate for non-constant τ_i spacing [19], their results are thus likely to be less appropriate and accurate than those of the PMO, which takes proper account of variable spacing. Fourth, the Ref. [13] condition for changing the value of M is evidently less effective for the PMW approach than that used for determining the most appropriate M value using the PMO. For example, out of 1000 MC fits of the continuous distribution data, the authors of [13] found only 15 with their maximum value of $M = 6$, while PMO inversion yielded nearly a full 1000 converged fits with $M = 11$, the most appropriate choice (see Figs. 4 and 5). Further, the estimated values and uncertainties of the PMO $\{e_i, \tau_i\}$ parameters were orders of magnitude better than those of the PMW. Finally, the present results have demonstrated that the PMO is capable of estimating a useful number of accurate $\{e_i, \tau_i\}$ values, while the NTRM can yield many more continuous-distribution points at the cost of decreased accuracy and inadequate resolution of closely spaced discrete DRT lines.

REFERENCES

1. C. W. Groetsch, *The Theory of Tikhonov Regularization for Fredholm Equations of the First Kind* (Pitman, Boston, 1984).
2. J. R. Macdonald, Power-law exponents and hidden bulk relaxation in the impedance spectroscopy of solids, *J. Electroanal. Chem*. **378**, 17 (1994).
3. B. A. Boukamp and J. R. Macdonald, Alternatives to Kronig–Kramers transformations and testing, and estimation of distributions, *Solid State Ionics* **74**, 85 (1994).
4. J. R. Macdonald, Exact and approximate nonlinear least-squares inversion of dielectric relaxation spectra, *J. Chem. Phys*. **102**, 6241 (1995).
5. J. R. Macdonald, Solution of an "impossible" diffusion-inversion problem, *Comput. Phys*. **9**, 546 (1995).
6. J. R. Macdonald, Analysis of dispersed, conducting-system frequency-response data, *J. Non-Cryst. Solids* **197**, 83 (1996); erratum, *J. Non-Cryst. Solids* **204**, 309 (1996). [G_D in Eq. (A2) should be G_{CD}, the present G_1 quantity.]
7. J. R. Macdonald, Analysis of immittance spectroscopy data: Model comparisons, universality, and estimation of distributions of activation energies, in *Electrically Based Microstructural Characterization, Proceedings, Fall meeting, November 1995* (Materials Research Society, Pittsburgh, PA, 1996), Vol. 411, p. 71.
8. J. R. Macdonald, The Ngai coupling model of relaxation: Generalizations, alternatives, and their use in the analysis of non-Arrhenius conductivity in glassy, fast-ionic materials, *J. Appl. Phys*. **84**, 812 (1998). [The word "out" in the third line from the bottom of the first column on p. 820 should be "but."]
9. J. R. Macdonald, Dispersed electrical-relaxation response: Discrimination between conductive and dielectric relaxation processes, *Braz. J. Phys*. **29**, 332 (1999).
10. J. R. Macdonald, Critical examination of the mismatch-and-relaxation frequency-response model for dispersive materials, *Solid State Ionics* **124**, 1 (1999).
11. D. Maier, P. Hug, M. Fiederle, C. Eiche, D. Ebling, and J. Weese, High resolution method for the analysis of admittance spectroscopy data, *J. Appl. Phys*. **77**, 3851 (1995).
12. J. Winterhalter, D. G. Ebling, D. Maier, and J. Honerkamp, An improved analysis of admittance data for high resistivity materials by a nonlinear regularization method, *J. Appl. Phys*. **82**, 5488 (1997).

13. J. Winterhalter, D. G. Ebling, D. Maier, and J. Honerkamp, Analysis of admittance data: Comparison of a parametric and a nonparametric method, *J. Comput. Phys*. **153**, 139 (1999).
14. J. R. Macdonald and L. D. Potter, Jr., A flexible procedure for analyzing impedance spectroscopy results, *Solid State Ionics* **23**, 61 (1987). [This work describes an earlier version of LEVM, then called LOMFP. The latest version of the LEVM, V. 7.1, may be obtained at no cost from Solartron Instruments, Victoria Road, Farnborough, Hampshire, GU147PW, England. Both the extensive manual, of more than 150 pages, and the program (including Fortran source code) may be downloaded by accessing http://www.physics.unc.edu/∼macd/.]
15. J. R. Macdonald and W. J. Thompson, Strongly heteroscedastic nonlinear regression, *Comm. Statist. Simulation Comput*. **20**, 843 (1991). [This work provides more background on LEVM and its capabilities, and the LEVM manual provides further definitive information.]
16. D. L. Losee, Admittance spectroscopy of impurity levels in Schottky barriers, *J. Appl. Phys*. **46**, 2204 (1975).
17. C. Elster and J. Honerkamp, The role of the error model in the determination of the relaxation time spectrum, *J. Rheol*. **36**, 911 (1992).
18. J. R. Macdonald, Comparison and application of two methods for the least squares analysis of immittance data, *Solid State Ionics* **58**, 97 (1992).
19. J. R. Macdonald, Some new directions in impedance spectroscopy data analysis, *Electrochim. Acta* **38**, 1883 (1993). [See the Appendix of this paper.]
20. J. R. Macdonald, Impedance spectroscopy: Old problems and new developments, *Electrochim. Acta* **35**, 1483 (1990).
21. W. J. Thompson, *Atlas for Computing Mathematical Functions* (Wiley, New York, 1997), p. 194.
22. J. R. Macdonald, Relaxation in systems with exponential or Gaussian distributions of activation energies, *J. Appl. Phys*. **61**, 700 (1987). [The numerator of the integrand in Eq. (20) should appear as $\exp[-(y/\xi)^2]$.
23. J. R. Macdonald, Linear relaxation: Distributions, thermal activation, structure, and ambiguity, *J. Appl. Phys*. **62**, R51 (1987).
24. J. Honerkamp, *Statistical Physics* (Springer-Verlag, Berlin/Heidelberg/New York, 1998), p. 291.
25. J. R. Macdonald, Accurate fitting of immittance spectroscopy frequency-response data using the stretched exponential model, *J. Non-Cryst. Solids* **212**, 95 (1997). [The symbol σ_0 should be removed from the right end of Eq. (12); Eq. (7) in this work does not apply to Eqs. (3) and (4) when $\rho_{C\infty} \neq 0$ (see Ref. [6] above); and the word "frequency" in the third line from the bottom of the second column of p. 111 should be "temperature."
26. J. R. Macdonald, Limiting electrical response of conductive and dielectric systems, stretched-exponential behavior, and discrimination between fitting models, *J. Appl. Phys*. **82**, 3962 (1997).
27. J. R. Macdonald, Comparison of the universal dynamic response power-law fitting model for conducting systems with superior alternative models, submitted for publication.
28. J. R. Macdonald, Restriction on the form of relaxation-time distribution functions for a thermally activated process, *J. Chem. Phys*. **36**, 345 (1962).
29. J. R. Macdonald, J. Schoonman, and A. P. Lehnen, The applicability and power of complex nonlinear least squares for the analysis of impedance and admittance data, *J. Electroanal. Chem*. **131**, 77 (1982).
30. M. Baumgärtel and H. H. Winter, Determination of the discrete relaxation and retardation time spectrum from dynamic mechanical data, *Rheol. Acta* **28**, 511 (1989).